

## **Heterometal doping on nickel selenide corrugations for solar-assisted electrocatalytic hydrogen evolution**

*Weiwu Chen,<sup>a</sup> Zhaojun Qin,<sup>\*a</sup> and Zhiming M. Wang<sup>\*a,b</sup>*

<sup>a</sup>Yangtze Delta Region Institute (Huzhou), University of Electronic Science and Technology of China, Huzhou 313001, China.

<sup>b</sup>Institute of Fundamental and Frontier Sciences, University of Electronic Science and Technology of China, Chengdu 610054, China

<sup>\*</sup>Corresponding authors.

Email: ZjQin@csj.uestc.edu.cn (Z. Q.), zhmwang@uestc.edu.cn (Z. M. W.).

## Experimental

### Materials

Ni foam (thickness: 1.6 mm), selenium powder (Se,  $\geq 99.5\%$ , Sigma-Aldrich), manganese acetate tetrahydrate ( $\text{C}_4\text{H}_6\text{MnO}_4 \cdot 4\text{H}_2\text{O}$ ,  $\geq 99\%$ , Sigma-Aldrich), cobalt (II) nitrate hexahydrate ( $\text{Co}(\text{NO}_3)_2 \cdot 6\text{H}_2\text{O}$ ,  $\geq 98\%$ , Sigma-Aldrich), iron (III) nitrate nonahydrate ( $\text{Fe}(\text{NO}_3)_3 \cdot 9\text{H}_2\text{O}$ ,  $\geq 98\%$ , Sigma-Aldrich), potassium hydroxide (KOH, 50% w/v, Alfa Aesar), graphite foil (Alfa Aesar), and Pt wire (CH Instrument) were used. Deionized water (resistivity:  $18.2 \text{ M}\Omega \text{ cm}$ ) was used for all of the aqueous solutions.

### Characterization

X-ray diffraction (XRD, PANalytical X'pert PRO diffractometer with a Cu Ka radiation source), X-ray photoelectron spectroscopy (XPS, PHI Quantera SXM scanning X-ray microprobe), scanning electron microscopy (SEM, LEO 1525) coupled with energy-dispersive X-ray spectroscopy (EDS), and transmission electron microscopy (TEM, JEOL 2010F) coupled with EDS were employed.

### Electrochemical measurements

All electrochemical performance parameters were tested in an alkaline solution of 1 M KOH using a three-electrode electrochemical station. Graphite foil and a Hg/HgO electrode served as the counter electrode and the reference electrode, respectively. All potentials were converted to a reversible hydrogen electrode (RHE) by the Nernst equation ( $E_{\text{RHE}} = E_{\text{Hg/HgO}} + 0.0591 \text{ pH} + 0.098$ ) and all measurements were conducted with iR compensation. The polarization curves were tested by sweeping the potential

from 0.065 to -0.325 V *vs.* RHE at a rate of 2 mV s<sup>-1</sup>. The cyclic voltammetry (CV) curves were conducted from 0.1 to 0.2 V *vs.* RHE at different rates. Electrochemical impedance spectroscopy (EIS) was performed at -150 mV *vs.* RHE from 100 KHz to 10 mHz with an amplitude of 10 mV.

## Supplementary Figures

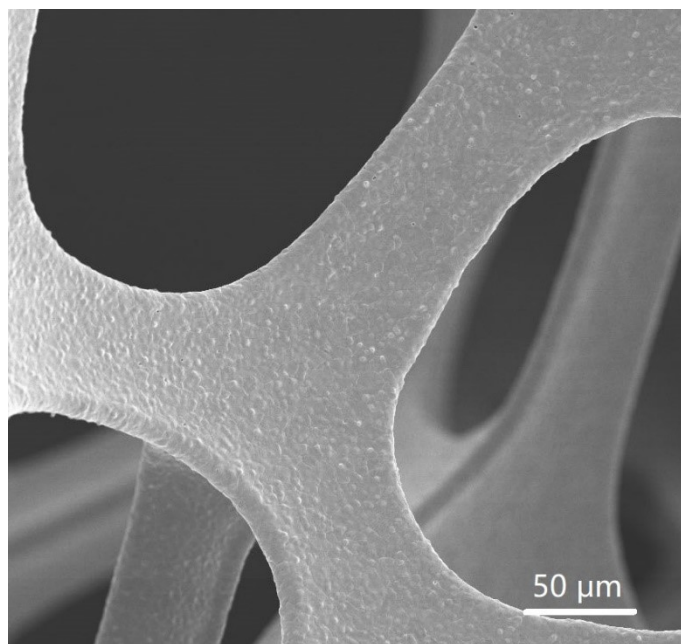


**Fig. S1** SEM image of Ni foam.

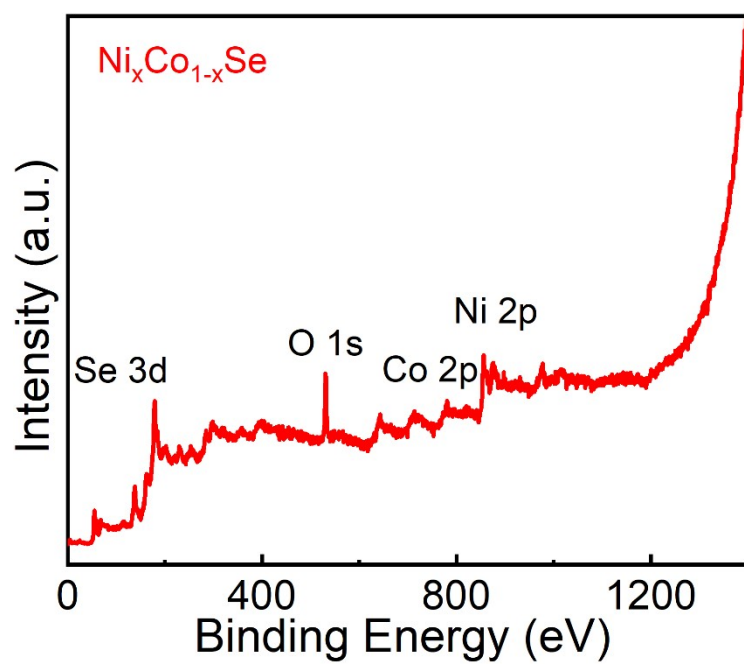


**Fig. S2** XPS spectra of  $\text{Ni}_{1-x}\text{Co}_x\text{Se}$ .

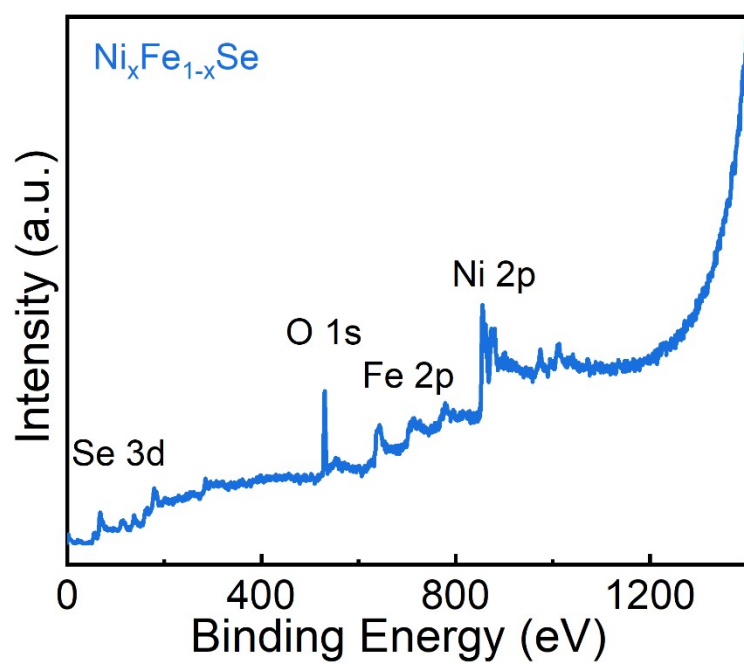


**Fig. S3** XPS spectra of  $\text{Ni}_{1-x}\text{Fe}_x\text{Se}$ .

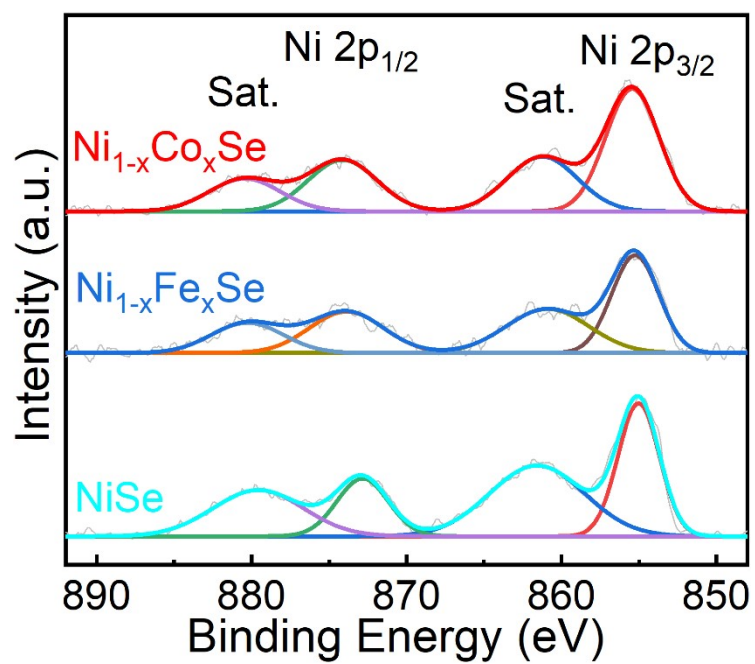


**Fig. S4** High-resolution XPS spectra of Ni 2p in  $\text{Ni}_{1-x}\text{Co}_x\text{Se}$ ,  $\text{Ni}_{1-x}\text{Fe}_x\text{Se}$  and  $\text{NiSe}$ .

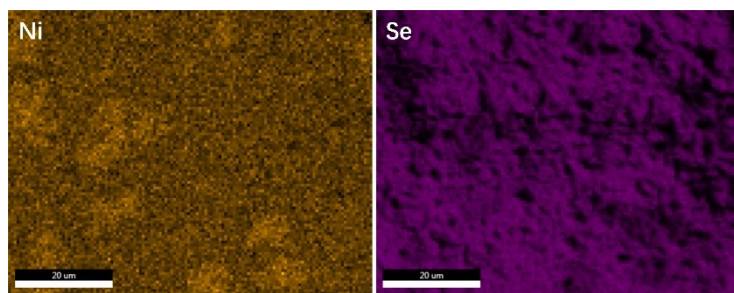


**Fig. S5** EDS mapping images of Ni and Se in  $\text{Ni}_{1-x}\text{Co}_x\text{Se}$  from SEM.



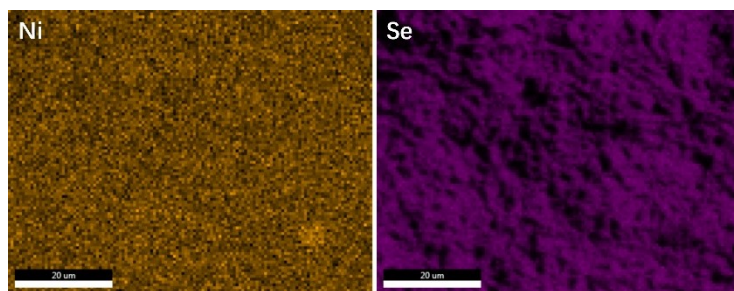


**Fig. S6** EDS mapping images of Ni and Se in  $\text{Ni}_{1-x}\text{Fe}_x\text{Se}$  from SEM.

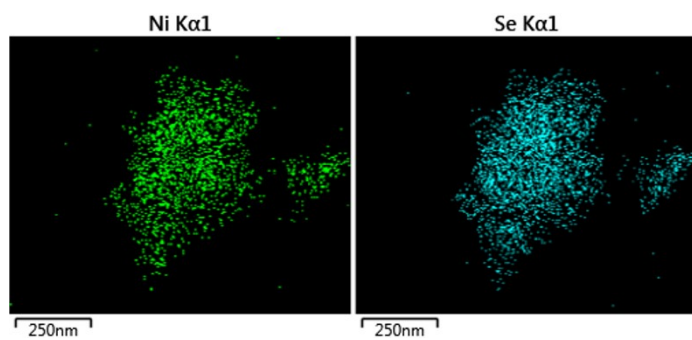


**Fig. S7** EDS mapping images of Ni and Se in  $\text{Ni}_{1-x}\text{Co}_x\text{Se}$  from TEM.

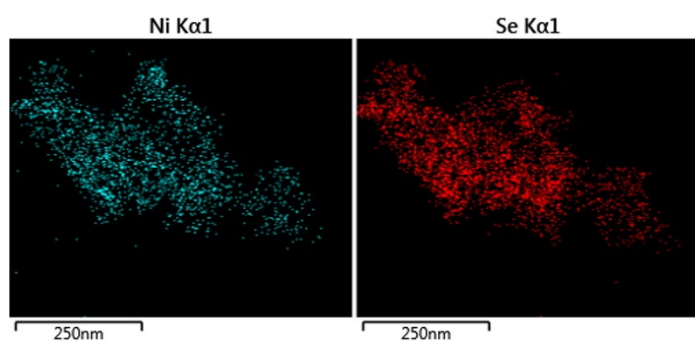


**Fig. S8** EDS mapping images of Ni and Se in  $\text{Ni}_{1-x}\text{Fe}_x\text{Se}$  from TEM.

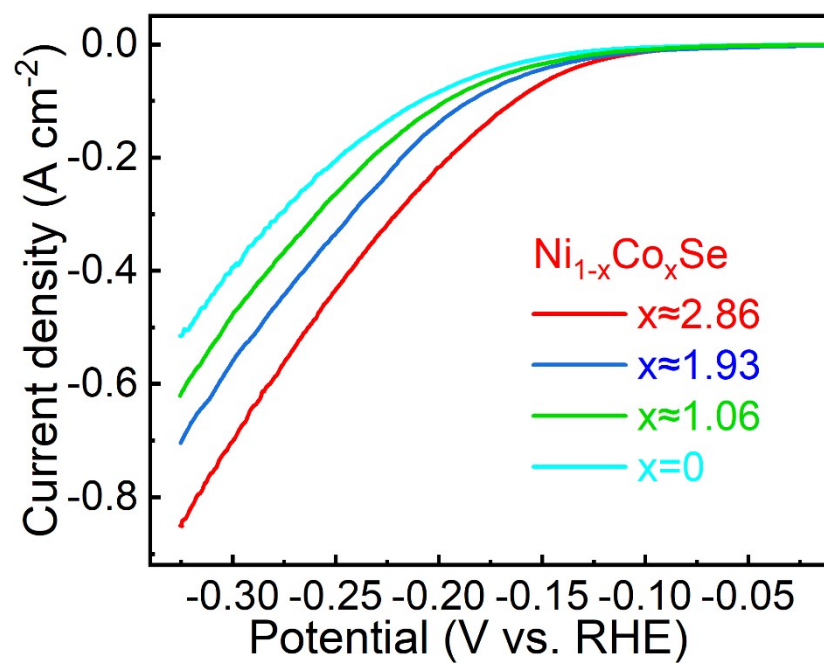


**Fig. S9** Polarization curves of the  $\text{Ni}_{1-x}\text{Co}_x\text{Se}$  samples with different content of Co in base.

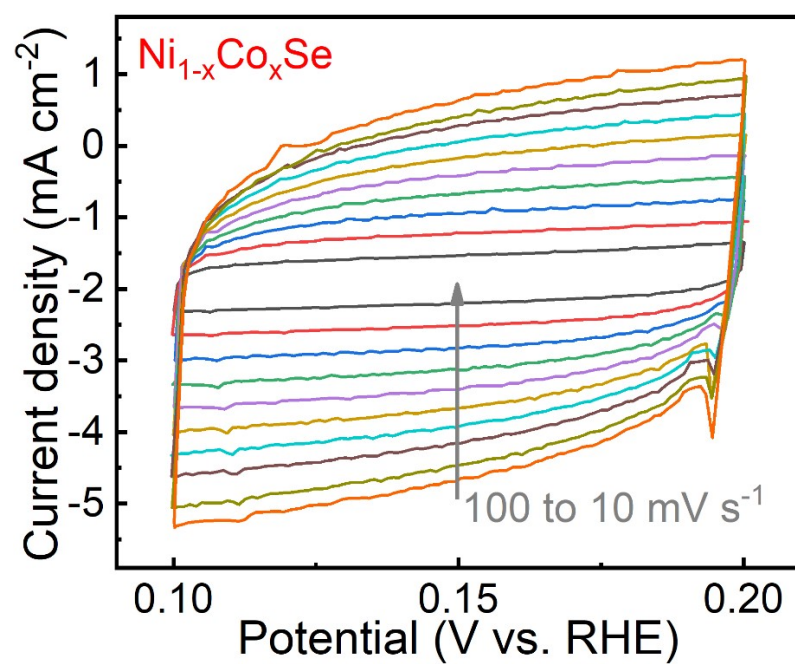


**Fig. S10** CV curves recorded for  $\text{Ni}_{1-x}\text{Co}_x\text{Se}$  electrodes over the potential range between 0.1 and 0.2 V vs. RHE at different rates in base.

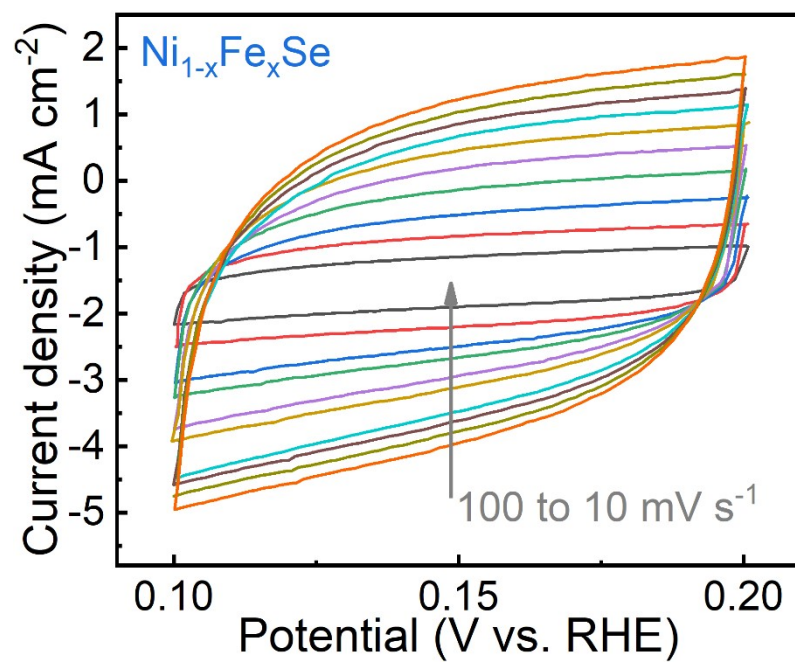


**Fig. S11** CV curves recorded for  $\text{Ni}_{1-x}\text{Fe}_x\text{Se}$  electrodes over the potential range between 0.1 and 0.2 V vs. RHE at different rates in base.

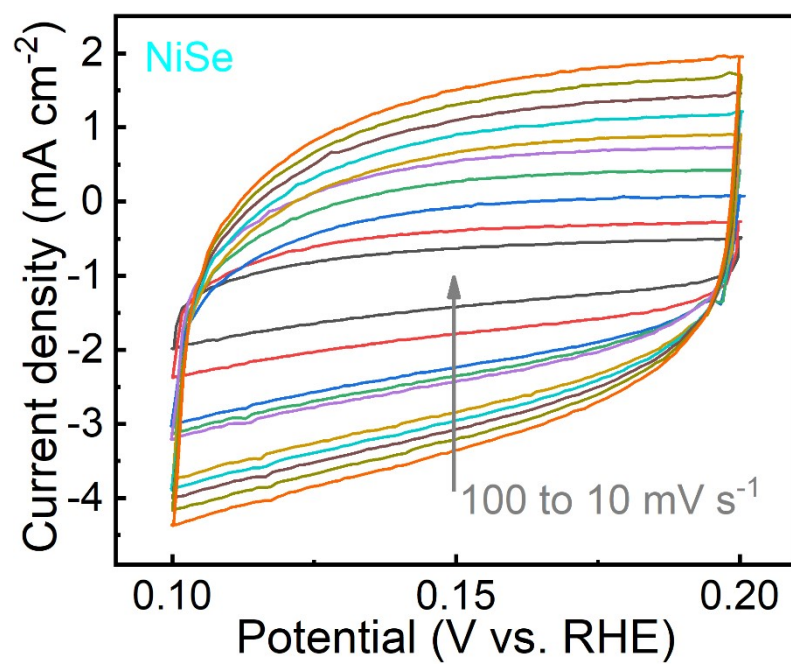


**Fig. S12** CV curves recorded for NiSe electrodes over the potential range between 0.1 and 0.2 V vs. RHE at different rates in base.

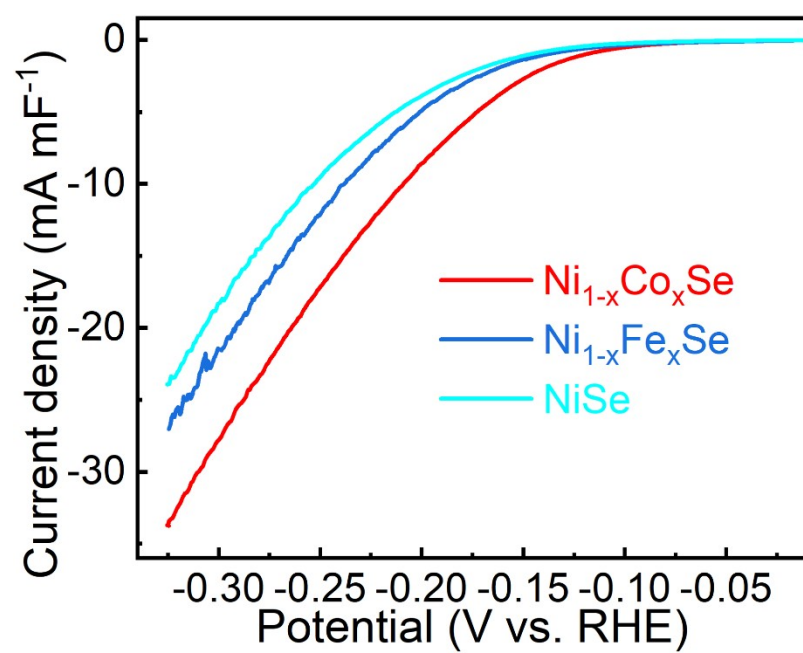


**Fig. S13** Normalization of the current based on the linear sweep voltammetry (LSV) curves.



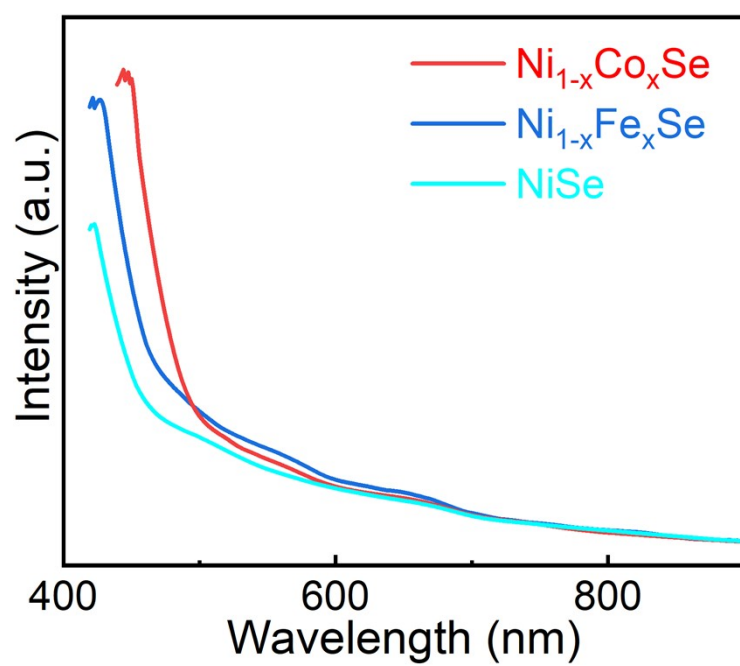


**Fig. S14** Normalization of the current based on the linear sweep voltammetry (LSV) curves.

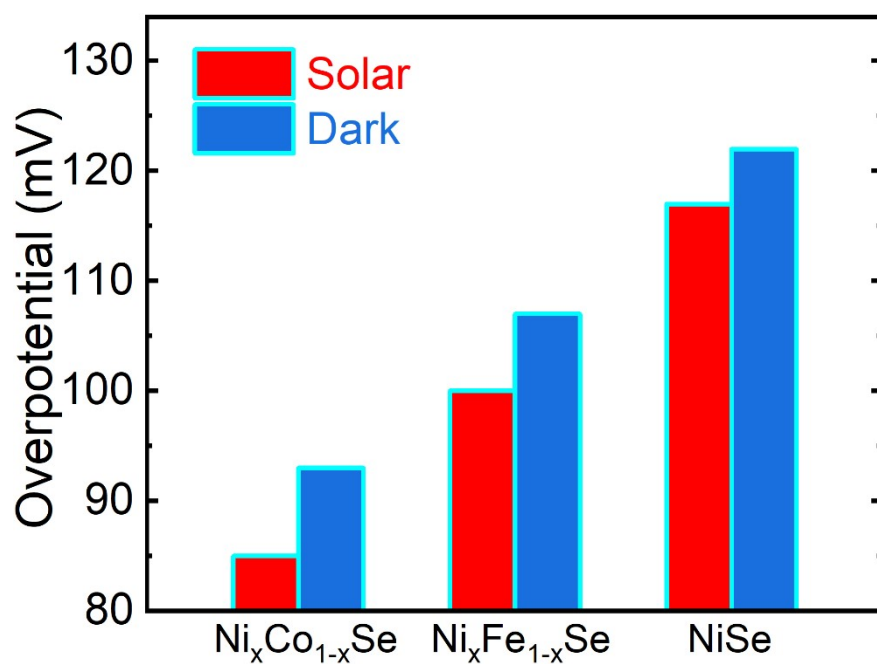


**Fig. S15** Overpotentials of different catalysts with and without illumination at current densities of  $10 \text{ mA cm}^{-2}$ .

## Supplementary Tables

**Table S1** Comparison of the HER performance between  $\text{Ni}_{1-x}\text{Co}_x\text{Se}$  and other previously reported NiSe-based catalysts in alkaline conditions. Here  $\eta_{10}$  is the overpotential at a current density of  $10 \text{ mA cm}^{-2}$ .

Catalyst	$\eta_{10}$ (mV)	Tafel slope (mV $\text{dec}^{-1}$ )	Source
$\text{Ni}_{1-x}\text{Co}_x\text{Se}$	93	68.2	This work
NiSe/Ni foam	96	120	Angew. Chem. Int. Ed. 2015, 54, 9351
NiSe	~150	76.6	Electrochim. Acta 2017, 224, 412
NiSe- $\text{Ni}_{0.85}\text{Se}$ /carbon paper	101	74	Small 2018, 14, 1800763
$\text{MoSe}_2$ -NiSe/carbon nanosheets	180	80.6	Carbon 2018, 139, 1
Two-tiered NiSe	177	58.2	Adv. Energy Mater. 2018, 8, 1702704
NiSe/ $\text{Ni}_3\text{Se}_2$ /Ni foam	92	101.2	Adv. Mater. Interfaces 2018, 5, 1701507
$\text{Fe}_{7.4\%}$ -NiSe	163	71.4	J. Mater. Chem. A 2019, 7, 2233